DAS - Acoustical Measurements Inside Different Environments

Finn Reikowski, Max Görler, Ivor Nissen

Bundeswehr Technical Center for Ships and Naval Weapons, Maritime Technology and Research, Eckernförde, Germany

FinnReikowski@Bundeswehr.org, MaxGoerler@Bundeswehr.org, IvorNissen@Bundeswehr.org

Introduction

The sea bottom of coastal waters like the Baltic Sea is covered by a web of power and communication cables. Recent advances in Distributed Acoustic Sensing (DAS) have made it feasible to transform each of these subsea cables into extended and close-meshed sensor arrays.

DAS measures microscopic changes in the optical length of the fiber, and is therefore sensitive to changes in the fiber strain induced by acoustic waves. Thus, a DAS system converts a subsea cable into a long (∼100 km) virtual hydrophone array with high spatial resolution (∼10 m). Since the sensitivity of DAS reaches down into the sub-Hz range it can adopt the role of a pressure sensor at the same time.

We present how DAS can be used to measure acoustics in different environments. Cables with different internal structures at water depths ranging from 10 m to 1500 m, embedded in sea bottoms including mud and sand, were investigated. The overall goal is to obtain a physical understanding how environmental parameters, like weather conditions and sea bottom structure, but also the structure of the cable itself affect the measurement performance. Ultimately, this will make it possible to establish propagation models in the future.

Experimental Methods

Distributed acoustic sensing uses optical fibers, commonly used for telecommunication, as extended sensors. A range of different methods have evolved, but we will focus on differential phase DAS (dΦ-DAS)[1], which has been used in our studies. This section aims to provide a simple introduction to this method, a more complete picture can be found in the literature[2].

Figure 1 shows the simplified functional principle of dΦ-DAS. The DAS interrogator, which is connected to the sensing fiber, consists of three main building blocks: a pulsed laser, a circulator and a phase detector. The laser produces very short pulses with a pulse length of a few meters and a long coherent length. After passing the circulator, the laser pulse enters the fiber. Due to Rayleigh backscattering, a very small fraction of the laser pulse is scattered back towards the circulator at all positions along the fiber. The circulator directs the backscattering signal to a detector which measures its phase $\phi(x)$. Since the light pulse travels through the fiber with a known speed v given by $v = c/n$, where c is the vacuum speed of light and n is the refractive index of the fiber material, the location from which the detected signal was received can be calculated from the travel time. This way we obtain the phase $\phi(x)$ for all locations in the fiber. Next, the phase differences $\Delta\phi(x)$ between intervals separated by the distance L_G, known as the gauge length, are calculated for all locations along the fiber.

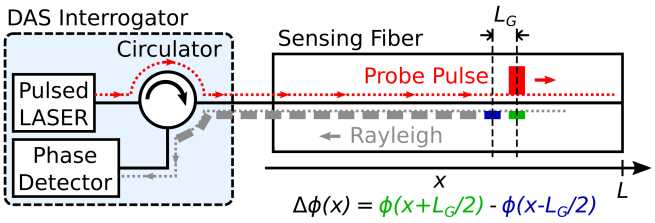

Figure 1: Simplified principle of dΦ-DAS. A laser probe pulse (red rectangle, dashed line indicating path) is coupled into the sensing fiber via a circulator. At all locations in the fiber a tiny fraction of the light is scattered back towards the circulator via Rayleigh scattering (grey rectangles, dashed line indicating path). The circulator propagates the back scattered signal to a detector measuring its phase $\phi(x)$. Once the detector received the last backscattering signal, the next probe pulse can be emitted. The phase difference $\Delta\phi(x)$ calculated for cable sections separated by the gauge length L_G is sensitive to the local fiber strain.

If the fiber is completely unperturbed, all $\Delta\phi(x)$ will remain constant for subsequent laser pulses. However, if the fiber is strained locally, the refractive index of the material at that location will be modified slightly. This leads to a change in the observed phase difference $\Delta\phi$ at that location. Therefore, dΦ-DAS is sensitive to changes in the local fiber strain, which can be induced by several mechanisms including temperature, pressure and other mechanical waves. In this work we will focus on the effect of pressure changes. By monitoring the evolution of $\Delta\phi(x)$ as a function of time, we can resolve both slow varying pressure (static) and fast varying pressure (acoustics).

The acoustic bandwidth, that can be achieved with this method, is determined by the laser pulse rate f_{pulse}. The maximum pulse rate, that can be used, is given by the time it takes until the backscattering signal from the far end of the fiber has arrived at the detector. It is mainly restricted by the speed of light in the fiber material and the length L of the investigated fiber and is given by:

$$f_{pulse} = \frac{1}{2L}\frac{c}{n} \approx \frac{100\,\mathrm{kHz}}{L/\mathrm{km}}. \qquad (1)$$

In this expression the factor 2 appears because we have to consider the forward path of the probe pulse and the return path of the backscattering signal. By inserting values for the typical refractive index n and the speed

of light in vacuum c we obtain the approximate expression, which provides a good rule of thumb. This condition ensures that the backscattering signal received in the phase detector always originates from a single pulse and thus from a single position in the fiber. In practice this condition can be relaxed. If we consider a fiber with a length of 100 km, Equation 1 allows a maximum pulse rate $f_{pulse} = 1\,\text{kHz}$. If we increase the pulse rate to $f_{pulse} = 2\,\text{kHz}$, signals from the current pulse at position x will overlap with signals from position $x + 50\,\text{km}$ of the previous pulse. With a fiber loss of approximately 0.2 dB/km the signal from the previous pulse will be weaker by $2 \cdot 50\,\text{km} \cdot 0.2\,\text{dB/km} = 20\,\text{dB}$. Therefore, the signal from the current pulse will be only slightly effected by the previous pulse and a relaxation of Equation 1 is possible for sufficiently long cables.

Experiments have been performed at different cables in different environments. Fundamental tests have been carried out at the WTD 71 test station in Aschau. At the test site a bundle of three different fiber optic cables was installed at the sea bottom parallel to existing pressure sensor- and hydrophone-arrays. At the position of the reference sensors the water depth is approximately 22 m.

Further measurements were performed at two different operational subsea cables: one in the Baltic Sea (2018) and one in the Atlantic Ocean (2024). For most of the experiments shown in this work the research vessel HELMSAND (MMSI = 211212220, length = 56.5 m, width = 10.8 m, draft = 3.3 m) was used.

Results

In order to understand how data obtained with DAS in the maritime environment compares with data from established sensors, i.e. pressure sensors and hydrophones, we performed measurements at our test station Aschau.

Figure 2a shows the differential phase data that was obtained while the vessel HELMSAND crossed the cable perpendicular with a speed of 14 kn. Since the test cable was quite short, we used a high pulse rate of $f_{pulse} = 10\,\text{kHz}$. A signature of the vessel is clearly visible and strongly resembles the expected pressure signature at the center of the crossing position. Blue and red colors indicate regions with positive and negative differential phase with respect to a reference value, which was obtained by subtracting a linear offset from the data. This linear offset was calculated for all spatial channels independently and was found by calculating the average value of the first and last 10 s of data and calculating a straight line between these values. Adding a constant offset for each channel is always necessary since the value of each channel will start at zero due to the differential nature of the measurement. The constant offset ensures that the background (water surface waves) oscillate around the same reference level of zero. By using a linear offset instead, we also reduce the effect of drift.

The bow and stern waves of the vessel can be seen as red patches around the center position ($x = 0\,\text{m}$) at time $t = -5\,\text{s}$ and $t = 5\,\text{s}$. The central blue patch corresponds

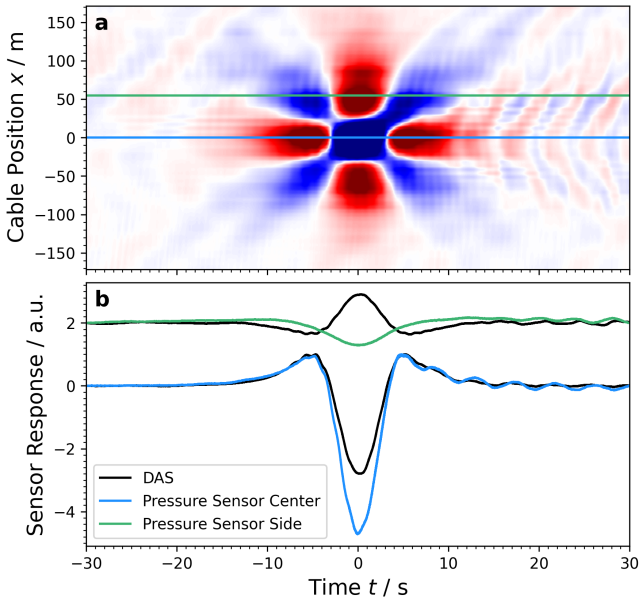

Figure 2: HELMSAND crossing the fiber with 14 kn. The center of the vessel is located at cable position $x = 0\,\text{m}$ at time $t = 0\,\text{s}$. a) shows the raw differential phase data, where red and blue colors correspond to negative and positive differential phase values, respectively. b) compares the DAS response and the response of pressure sensors at two locations marked with blue and green lines in a). At $x = 0\,\text{m}$ the data is in very good qualitative agreement. The bow (stern) waves at $t = -5\,\text{s}$ ($t = 5\,\text{s}$) and the negative peak underneath the ship appear in the same expected location. At $x = 50\,\text{m}$ a similar shape is observed, but the sign of the changes is inverted.

to a region of under-pressure underneath the hull of the vessel, caused by an increase in dynamic pressure while the vessel crosses the cable. Interestingly, a similar pattern but with the opposite sign is observed at distances >30 m away from the center on both sides. Even smaller details, like the backwash that can be seen in the whole region after $t = 10\,\text{s}$, are picked up with this method. The characteristic V-shaped pattern of the waves spreading out behind the vessel is clearly visible.

Figure 2b compares the differential phase data shown in a) with data from pressure sensors obtained at two different positions directly underneath ($x = 0\,\text{m}$) and 50 m besides the center of the ship. To simplify comparison of the two datasets, the maximum values of the curves at $x = 0\,\text{m}$ were scaled to one. The same scaling factors obtained for the central curves were used to scale the data at $x = 50\,\text{m}$.

For the central position at $x = 0\,\text{m}$ both curves show the same behaviour apart from a few details. The bow and stern waves, the region of under-pressure as well as the waves of the backwash appear at the same location demonstrating that the DAS signal is indeed caused by the pressure signature of the ship. However, smaller differences in the magnitude of the central negative peak and the amplitude of the oscillations in the backwash are visible.

The differences in the signals at $x = 50\,\text{m}$ are more striking. Here the signals show similar features, but with a

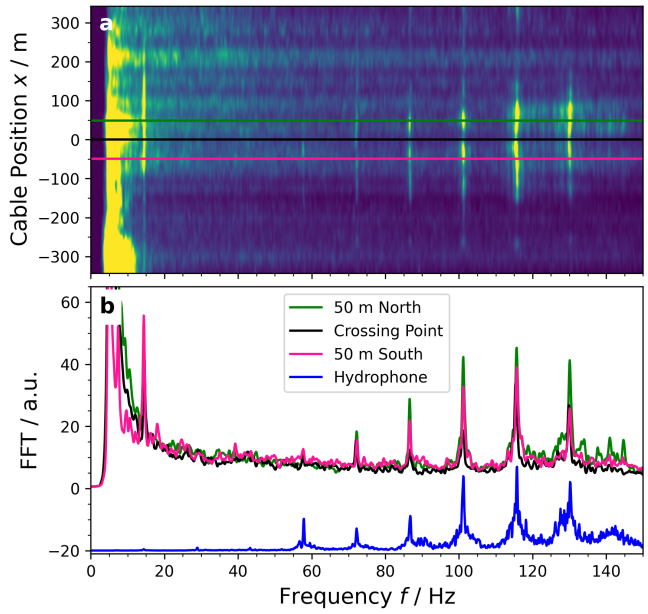

Figure 3: FFT of a 10 s interval of phase data after the HELMSAND crossed the fiber. Before calculating the FFT, a highpass filter with a cutoff frequency of 5 Hz was applied to the phase data. a) Spectra for all channels in a range of ±340 m around the crossing location are shown. A line spectrum can be clearly identified. b) Spectra at selected positions along the fiber along with a reference spectrum measured with a hydrophone. The same lines that are visible in the hydrophone data are also visible in the DAS data.

flipped sign. This suggests that the origin of the signal is still the pressure signature of the vessel. However, the pressure field cannot be directly obtained from the observed fiber response and a more elaborate treatment is required. A further complication is that contrary to a conventional pressure sensor, which measures the pressure at a small and well-defined position in space, DAS is an extended sensor which measures the differential phase between two cable sections separated by the gauge length L_G.

Despite these differences, the sensitivity of DAS with respect to pressure changes is very similar to classical sensors. This demonstrates that DAS can provide a very useful pressure sensor array, especially when the detection of pressure changes is more important than the accurate determination of actual pressure values. Figure 2 reveals that the dominating part of the DAS signal is caused by static pressure. By calculating the FFT of the differential phase data we can investigate the sensitivity towards higher frequencies in the acoustic domain.

Figure 3 shows the FFT of the same dataset, calculated over an interval with a duration of 10 s, starting after the vessel passed the cable. Before calculating the FFT, the differential phase data was filtered using a high-pass filter with a cutoff frequency of 5 Hz to reduce the dominating pressure signal. Figure 3a shows the spectra calculated for all DAS channels in a range of ±340 m around the crossing location. A clear line spectrum with a fundamental frequency and harmonics is visible. The intensity of the lines in the different channels varies significantly. Not only the intensity level differs for individual channels, but also the relative intensity of the lines. Figure 3b shows spectra at three different locations marked with black, green and pink lines in Figure 3a. The figure also shows a reference signal recorded with a hydrophone (blue line). The location of the lines are in excellent agreement, but the relative intensity of the lines is different. This is not surprising, as the relative intensity distribution of the lines for different DAS channels shows a complex behaviour.

When considering the capability of DAS, it is particularly interesting to look at the first line of the spectrum. While this line is barely visible on this linear scale in the spectrum of the hydrophone, it is clearly visible in the DAS spectrum where it is the most intense line. However, despite this difference in signal strength, the signal-to-noise ratios of the two peaks are comparable. The interesting feature of DAS is that it covers the full frequency range down into the sub-Hz pressure domain.

At the higher end of the spectrum DAS is significantly less sensitive than hydrophones for several reasons. The most obvious reason is the lower sampling rate, which is the dominating effect especially for long cables (see Equation 1) and sets a strict upper frequency limit. Another reason is that with increasing frequency the acoustic wavelength λ becomes much smaller than the fiber section used for a single channel. With a sound velocity in water $v \approx 1500\,\mathrm{m/s}$ and the wavelength given by $\lambda(f) = v/f$, the wavelength at 100 Hz is $\lambda(100\,\mathrm{Hz}) \approx 15\,\mathrm{m}$. In these experiments we used a gauge length $L_G = 10\,\mathrm{m}$ so at a frequency of 1 kHz the wavelength $\lambda(1\,\mathrm{kHz}) \approx 1.5\,\mathrm{m}$ is already much smaller than the used section of the fiber. However, especially at low frequencies, which are important in the detection of propeller noise, DAS can provide a very useful detector.

In order to understand how operational telecommunication cables compare to our controlled environment we also performed measurements on two different subsea cables. Figure 4 shows a similar dataset as shown in Figure 3 recorded at a subsea cable in the Atlantic Ocean. The cable length was greater than 300 km which would according to Equation 1 only allow a sampling rate of around 300 Hz. However, as discussed above for sufficiently long cables the conditions on the maximum pulse rate can be relaxed and a pulse rate $f_{pulse} = 1\,\mathrm{kHz}$ was used for this measurement. It must be noted that a higher pulse rate not only increases the maximum frequency that can be resolved, but also increases the signal-to-noise ratio of the measurement. Therefore, it is always desirable to use the highest possible pulse rate.

Here the vessel HELMSAND crossed the cable at a water depth of ≈70 m with a speed of 13 kn. The line spectrum is clearly visible, but the variation of line intensity is much more pronounced. Some of the lines are visible even at a distance of 1 km from the crossing location. In addition to the line spectrum with the fundamental frequency and harmonics, an additional line around 60 Hz is visible. Since the vessel crossed the cable under an angle,

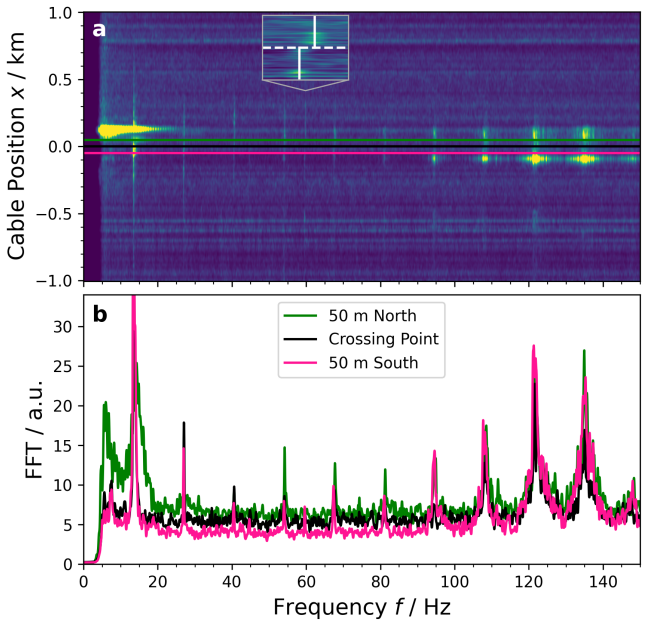

Figure 4: FFT of a 20 s interval of phase data after the vessel HELMSAND crosses an operational telecommunication cable in the Atlantic Ocean with a speed of 13 kn. The water depth was ≈70 m. A line spectrum around the crossing location is clearly visible. The inset in a) shows a closer view on one line visualizing an oppositional doppler shift at both sides of the crossing position.

a doppler shift between the spectra North and South of the crossing position can be observed. While this shift is barely visible on the green and pink spectra in b), the effect can be clearly seen in the inset in a) which shows a closer view on the line around 60 Hz. This doppler shift can be used to precisely determine the crossing location of the vessel which is otherwise more difficult since the spectrum is visible over a large range of the fiber. In particular, the brightest spots do not correspond to the exact crossing location but are significantly offset. Likewise, the doppler shift between the spectrum before and after the vessel crossed the cable can be used to precisely determine the crossing time. This demonstrates that DAS provides a very useful extended acoustic sensor which is well capable of detecting vessels. Pressure signatures of vessels could not be identified for this cable. There are several reasons for this. First, the water depth was significantly larger than in our test setup in Aschau. However, even at locations closer to the coast with comparable water depth no pressure signatures could be identified. The reason for this is most likely that the cable is buried in the seabed which attenuates the pressure.

Further measurements were conducted at a telecommunication cable in the Baltic Sea which was much shorter so that a pulse rate of $f_{pulse} = 2$ kHz was used. At this cable it was not only possible to detect acoustic signatures, but also pressure signatures of larger ships. Figure 5 shows the differential phase data while a cargo vessel with a length of 112 m and a width of 14 m crossed the cable with a speed of 11 kn at a water depth of approximately 20 m. For this vessel a pressure signature is clearly visible, but the signal is much weaker than for the reference

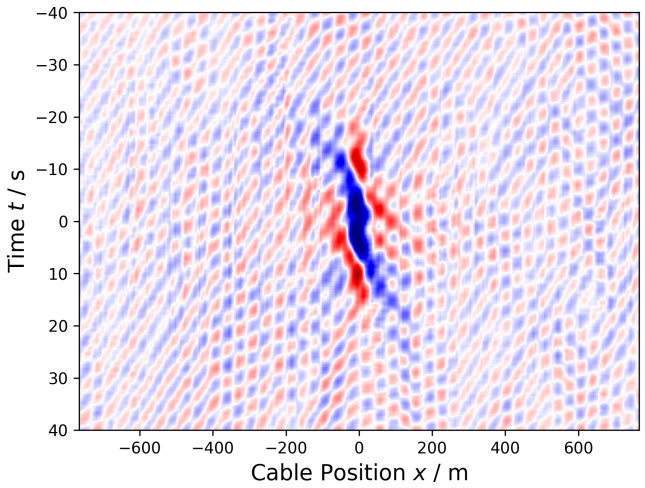

Figure 5: Differential phase data of a cargo vessel (length = 112 m, width = 14 m) crossing an operational telecommunication cable in the Baltic Sea at a water depth of ≈20 m. The pressure signature of the vessel is clearly visible but considerably less well-defined as in our reference measurements in Aschau (see Figure 2).

data in Aschau, especially when taking into account that the vessel is significantly larger. Similarly, the reason for this is most likely that the cable is buried in the seabed which attenuates the signal. This demonstrates that in principle subsea cables can also be used as extended pressure sensors, at least for stronger signals and especially in shallow waters.

Conclusions

We have shown how data obtained with dΦ-DAS in the maritime environment compares to conventional measurements with pressure sensors and hydrophones. It was shown that DAS is very sensitive to changes in the pressure with a sensitivity comparable to conventional pressure sensors. Although the sensitivity is similar, the response of the sensor is more complicated and cannot be directly translated into pressure. Comparing the DAS data with hydrophones in the frequency domain showed that similar spectra are produced although the frequency response is different. While DAS suffers at higher frequencies ≫100 Hz, it provides similar performance at the lower end of the spectrum covering the whole range into the sub-Hz pressure domain. It was demonstrated that both, the pressure sensing and the acoustic sensing capability of DAS, can be used to detect vessels crossing subsea cables.

References

[1] Z. Pan, K. Liang, Q. Ye, H. Cai, R. Qu, and Z. Fang.: Phase-sensitive OTDR system based on digital coherent detection, Optical Sensors and Biophotonics III (2011), 8311:0S-1

[2] A. H. Hartog: An Introduction to Distributed Optical Fibre Sensors, CRC Press, 2017